RSC Advances




ROYAL SOCIETY OF CHEMISTRY

www.rsc.org/advances

# A Universal Laser Marking Approach for Treating Aluminum Alloy Surface with Enhanced Anticorrosion, Hardness and Low Friction

Qiao-Xin Zhang,[†] Ming-Kai Tang,[†] Zheng Guo,[‡] Jin-Gui Yu,[†] Xue-Wu Li,[†] and Xing-Jiu Huang*[,†,‡]

[†]School of Mechanical and Electronic Engineering, Wuhan University of Technology, 122 Luoshi Road, Wuhan, 430070, P. R. China

[‡]Research Center for Biomimetic Functional Materials and Sensing Devices, Institute of Intelligent Machines, Chinese Academy of Sciences, Hefei, 230031, P. R. China

*Address correspondence to X.-J. Huang

E-mail: xingjiuhuang@iim.ac.cn (X.J.H)

Tel.: +86-551-5591142; fax: +86-551-5592420.

**ABSTRACT**

Lined and grating grooves have been fabricated on the large scale engineering Al alloy plate via a simple, convenient, efficient, and low cost laser marking method. Scanning electron microscopy (SEM) and X-ray photoelectron spectroscopy (XPS) are employed to characterize and analyze the microstructure and composition of as-prepared samples. The results demonstrate that regular and tailored roughness structures are successfully constructed on their surface. In addition, their roughness structures can be easily modulated. Furthermore, the corrosion resistances to seawater and tribological properties have been investigated. It indicates that the corrosion resistance, hardness and friction resistance of Al alloy surfaces treated by the laser marking approach are remarkably enhanced, which presents a great perspective application in the engineering field.



**KEYWORDS**

Laser marking approach, engineering material, aluminum alloy, anticorrosion, tribology

## INTRODUCTION

Aluminum (Al), especially for its alloy, has been widely applied in various fields including automobiles, medical, electrical and electronics and aerospace industries because of its high strength/weight ratio, unique conductivity of heat and electricity, non-ferromagnetic, nontoxic, good formability, and easily recyclable.[1-5] However, it is also accompanied with some intrinsic characteristics such as low hardness, poor wear resistance and poor corrosion resistance, which greatly limit their further applications.[1, 6-8] Therefore, it is very important to overcome the aforementioned disadvantages of Al and its alloy in the mechanical engineering field.

Aiming to the above mentioned issues, tremendous efforts have been made and various approaches have been developed over the past several decades. The typical strategy is to change the fine composition of its bulk and surface for Al alloy. Some metals including manganese (Mn), tin (Sn), molybdenum (Mo), lead (Pb), chromium (Cr), niobium (Nb), tungsten (W) and zirconium (Zr) have been employed as modifiers to improve the wear and corrosion resistance properties of Al alloy in some specific working conditions.[9-13] For example, Hukovic et al have investigated the electrochemical properties of the system Al-Mo alloy and found that the content of Mo can affect the corrosion resistance of the alloy.[14] The investigation of the mechanical of Al-Pb alloys and Al-Sn alloys indicated that the content of Sn and Pb could both change the friction coefficient of alloys.[15] However, these improvements are still limited owing to the low solid solubility (< 1 at %) between the doped metals and Al.[1] Surface modification as an alternative approach is a comprehensive concept considering the change of chemical and mechanical properties of the surface layer of metal materials.[16-21] Through depositing a coating on their surface, their corrosion and wear resistance could be enhanced.[22-25] For example, Fix et al have deposited a silica-zirconium based hybrid film with nanocontainers on Al alloy

(AA2024) to improve the ability of its corrosion resistance.[26] By electrical deposition, functionally graded (FG) nano-structured Ni-Co/SiC were coated on Al substrate to improved the wear resistance of the surface.[27] Furthermore, the corrosion and wear resistance of Al alloy can be improved by changing the surface compositions. For example, a composite layer is formed on the Al 6061-T651 alloy surface by stirring and mixing sub-micro-size $Al_2O_3$ and SiC particles into the surface. Compared with a non-processed Al surface, the composite surface exhibited substantial friction and wear reductions.[28] By forming compact Al-O-Si and Si-O-Si covalent bond network bridges with sulphide phases in the interface zone, Guo et al have produced bilayer silanisation film layer on AA2024-T3 alloy and prove that the corrosion resistance of Al alloy is improved remarkably.[29] Although various surface modifications have been successfully carried out, they still face some challenges including rigorously fabricated process, time-consuming and so on. More importantly, they cannot be performed in the large scale and most of the fabricated surface films are easily destroyed. Restricted by the aforementioned shortcomings, it is still desirable and necessary to develop simple, high efficient approaches with processing in the large scale to improve the wear and corrosion resistance of Al alloys.

Because of fast adaptability, high precision and cleanness of environment, the laser technology has been widely applied in various fields. Especially for the surface treatment, it can tailor the superficial properties and simultaneously maintaining the bulk properties.[30, 31] For example, by laser gas assisted melting, the metallurgical structure and microhardness of tungsten carbide surface have been changed and improved, respectively.[32] Furthermore, previous reports have demonstrated that a specific surface texture into a sliding contact surface can influence the coefficient friction of the surface.[33-35] For instance, Steinhoff et al have investigated the sheet-surface structure and find that different types of surface structure are able to affect the

tribological properties of the surface.[36] Initiated from this view, herein a rapid and one-step method of the laser marking approach has been employed to construct specific microstructure on Al alloy surface to improve its corrosion resistance, hardness and wear resistance simultaneously. This method is low cost, high efficient and facile operation in the large scale. Firstly, two typical patterns of lined and grating grooves have been fabricated on the Al alloy surface via the laser marking approach. Through optimizing the working parameters of the laser marking machine, roughness structures on the Al alloy surface can be accurately modulated. The corrosion resistance to seawater and tribological properties of the fabricated surfaces are carefully investigated. It is demonstrated that the corrosion resistance, hardness and friction resistance of Al alloy surface treated by the laser marking approach can be simultaneously enhanced, which shows a great perspective application in the engineering field.

## EXPERIMENTAL SECTION

**Materials.** The commercially available Al alloy (AA7075) plates were purchased from Alcan Alloy Products Company. Ltd (the chemical composition in mass percent: 0.4 Si, 1.2 Cu, 0.3 Mn, 2.1 Mg, 0.20 Cr, 5.1 Zn and the balanced Al). The plate was cut by wire cut electrical discharge machining in the form of 20 mm × 20 mm square pin. The surface of the cut samples were then ground to a surface roughness less than 0.05 μm and rinsed with ethanol and acetone.

**Laser marking treatment.** The surface of samples was treated under different processing parameters by a portable laser marking machine (YAG laser with a wavelength of 1064 nm, output power of 20 W). Different processing parameters included laser frequency, laser scanning speed and laser scanning times. The lined and grating grooves were made on the sample and the

angle of the grating patter was 90°. After treated, all the samples were cleaned twice in ultrasonic bath by alcohol and each for 10 min.

**Characterization.** The textured surfaces were observed by a Quanta 200 FEG Environmental scanning electronic microscopy (ESEM). X-ray photoelectron spectroscopy (XPS) analyses of the samples were conducted on a VG ESCALAB MKII spectrometer using an Mg Kα X-ray source (1253.6 eV, 120 W) at a constant analyzer. The Vicker's hardness of texture surface was measured using a HVS-1000 Vicker's hardness instrument with a load of 1 Kg and a dwell time of 8 s. Five tests were conducted and the mean value was given. The density of sintered specimens was determined by Archimedes' principle.

The tribological properties of the textured samples were measured with a HT-1000 ball-on-disk high temperature tribometer. The disk was made of the samples, and the counterpart ball was the commercial C45E4 steel ball with a diameter of 6 mm (600 HV, Ra 0.02 μm). Detailed experimental conditions of test were set as follows: rotation speed at 500 r/min, load of 1.65 N, at room temperature and time of 3 min.

## RESULTS AND DISCUSSION

The whole process of the laser marking approach is described in **Figure 1a**. During the marking process, the laser beam travels along a track which has been set up. As shown in **Figure 1b**, the polished Al alloy surface is rapidly heated and melted along the laser track. Then it will be vaporized and removed from the track, leading to the formation of grooves. Simultaneously, some melted part will be squeezed out from grooves due to the laser impact force and cool down rapidly to pile up together, leading to form many humps on the surface. This approach is not complicated nor does it use sophisticated equipment. Additionally, the process area just depends

on the area of plate of laser marking machine and there is no requirement for the thickness of materials. Therefore, it is quite easy to realize the large-scale treatment of the surface of Al alloy by expanding area of the plate of laser marking machine.

**Surface Topography**

As shown in **Figure 2a**, a typical Al alloy plate with a size of 230 mm × 230 mm × 60 mm is employed to treat by the laser marking machine. **Figure 2b**, **c** and **d** present SEM images of the untreated surface and as-prepared textured surface, respectively. For the untreated sample presented in **Figure 2b**, its surface is relatively smooth. Through the laser marking approach, it can be seen that the designed grooves patterns have been fabricated on their surfaces. **Figure 2c** and **2d** present the typical regular lined and grating patterns, respectively. Clearly, the spacing of their textures is uniform about 50 μm for lined and grating grooves, which is in good agreement with the designed pattern. However, due to the melted fusion deposition, some of lined textures flock together. From SEM image shown in **Figure 2c**, evidently many irregular micro-humps are formed along the lined distribution on the surface. For the grating pattern, the cross angle of the lined micro-humps is 90°, as presented in **Figure 2d**.

To better understand the effect of processing parameters, such as frequency, scanning speed and scanning times of the laser, the morphology of the treated grating grooves surface are investigated. SEM images of as-prepared samples are described in **Figure 3**. At the laser frequency of 5000 Hz, the melted degree of material decreases due to the decrease of laser stay time on the surface and laser displacement. As shown in **Figure 3a**, the melted material will form microstructure individually instead of flocking together, which is different from that shown in **Figure 2c** under the frequency of 2500 Hz. From the magnified SEM image shown in the inset of **Figure 3a**, it can be seen that the shape of milky protrusions are not uniform. When the

grating grooves surface is fabricated under a higher scanning speed of 150 mm/s, the distance between two beams of the laser increases consequently, resulting in the increase of the distance among the melted spots. It is difficult to flock together for the melted material around each melted spot. As clearly shown in the inset of **Figure 3b**, the milky protrusions turn to be more compact and uniform. When the scanning times increases to 2, from the high magnified SEM image inset in **Figure 3c** it can be easily found that the micro-humps become bigger and more regular than before. This phenomenon can be ascribed that the material of textured surface is melted and cooled down repeatedly with no effect to the grating grooves pattern. As continuously increase the scanning times to 4 (**Figure 3d**), the micro-humps turn to be more regular, while the diameter deceases. Based on the above results, the frequency and scanning speed of laser in contrast with scanning times would make great influence on the laser state (laser stay time, laser displacement and distance of each beam of laser) on the surface, which has a great effect on the construction of microstructure. Therefore, roughness structures on the surface can be accurately modulated by changing the laser frequency and scanning speed.

Besides the change of microstructure of the treated surface, the composition of the surface layer may be also changed under the instantaneously high temperature generated by the laser in air. In order to demonstrate this point, X-ray photoelectron spectroscopy (XPS) is performed to investigate the composition of the Al alloy surfaces. As shown in **Figure 4a**, it can be observed that oxygen, carbon, aluminum, magnesium, silicon are detected on untreated surface. As shown in **Figure 4e** and **4f**, the elements of zinc and copper are emerged after laser treatment, indicating that they are exposed from the bulk of Al alloy to form their precipitated phase on the surface. From the XPS spectra of Al 2p as shown in **Figure 4c**, it can be easily found that both the peaks at 72.4 and 74.7 eV can be detected for untreated surface. They are from the pure aluminum and

the oxidized aluminum, respectively. After the laser treatment, the peak at 72.4 eV disappeared, indicating that the pure aluminum is completely oxidized to $Al_2O_3$ on the surface under the high temperature induced by the laser. Interestingly, silicon is not detected on the surface as shown in **Figure 4d**, which may be attributed to the surface region completely covered with the oxide film and the new precipitated phase. All the C1s peaks are located at the same position (284.8 eV), which implicates that they come from the same contribution. Carbon is a kind of extremely sensitive element, therefore it is easy to detect by analyzing the XPS spectra. The carbon on the surface may come from the accumulated pollution during pre- and post- laser treatment. As shown in **Table 1**, it is apparent that the carbon content decreases significantly after laser treatment. For oxygen and aluminum, their contents dramatically increase. Additionally, because of the difference of microstructure on the surface, magnesium content of the textured surface decreases slowly with the increase of laser scanning times from 1 to 2 and keep the same level with the increase of laser scanning times from 2 to 4. Copper content has a slight increase when the laser scanning times increases to 2, then it decreases. Based on the above XPS results, it can be inferred that the laser marking treatment can change the composition of the surface layer, which will affect the properties of material. But the process parameters (frequency, scanning speed and scanning times) of laser marking have little effect on the composition of the surface. The thickness of the surface oxidized film ($Al_2O_3$) will increase after laser treatment, which may enhance the corrosion resistance of the surface. Furthermore, due to the aging strengthening process induced by laser treatment, zinc, copper and magnesium will be separated, leading to the formation of the precipitated phase on the surface, which may improve the hardness of Al alloy.

**Corrosion Resistance to Seawater**

Due to the wide applications of Al alloys on shipping and deep-diving submersible vehicles, the corrosion resistance to seawater of these Al alloys must be excellent.[37, 38] When the Al alloy contacts with the sea water, the Al alloy surface will directly suffer from the local corrosion.[1] In order to investigate the corrosion resistance to seawater of textured surface, a corrosion experiment was conducted by immersing the textured sample into seawater to imitate the actual situation of sample in seawater environment. The seawater was obtained from the coastal waters of China. The textured sample and the polished sample were immersed into seawater at room temperature.

Compared with the polished surface shown in **Figure 5a**, there is a large area black mark on the surface after immersing into seawater for 20 days and the surface with the black mark is uneven, which indicates that the oxidized film of the surface lost efficacy and the material surface reacted with seawater. **In Figure 5c**, the region of large area black mark is irregular, meaning that there are some defects on the surface of the polished sample and the integrity degree of the alloy oxidation film is affected by the defects. On the contrary, there is not any black mark on the surface of textured sample. Notably, the surface immersed into seawater for 20 days is almost the same as the previous surface shown in **Figure 5b**. Only some of black spots appeared on the edge of the surface (**Figure 5d**). It can be inferred that the black spots appeared on the edge of the surface is because that the edge of the surface and side surface are not treated by the laser. In order to further insight into the surface after immersing into the seawater, the surface of two samples were observed by SEM. As it shown in **Figure 5e**, it can be easily found that there are some blisters on the surface of the polished sample and they are random distributed on the surface. Due to the reaction between Al alloy and sea water, atomic hydrogen will diffuse into the material of the surface. As the atomic hydrogen aggregates in the material, the hydrogen

atoms become hydrogen molecule. With the increase of pressure of hydrogen, the material of the surface will deform and blistering will be induced on the surface. The hydrogen blistering means the surface suffers from the corrosion of seawater and the alloy oxidation film loses efficacy. The hydrogen blistering will weaken the performance of the material. Both hydrogen blistering (**Figure 5e**) and large area black mark (**Figure 5c**) observed on the polished surface indicate that the surface is corroded seriously by seawater after immersing into seawater for 20 days. Compared with the former, the textured surface has no change after immersing into the seawater for 20 days (**Figure 5f**), which indicates that the surface are not affected after corrosion experiment. The corrosion experiment proves that the corrosion resistance of textured surface treated by laser marking system is better than that of the polished surface. More importantly, compared with polished surface, the surface treated by laser marking has a long-term stability of performance in seawater, which will have an extensive application. Combining with the results of XPS, it can be concluded that the performance of corrosion resistance to seawater totally depends on the integrity degree and thickness of the alloy oxidation film on the alloy surface.

**Friction and Wear Properties of Textured Surface**

In order to investigate the friction resistance of the textured surfaces, tribological tests are conducted. Before tribological tests, the Vicker's hardness of textured surfaces treated by different processing parameters was measured (**Figure 6**). The hardness is an important parameter, which can affect the friction resistance of the surface. The hardness of smooth surface is about 185 HV. Therefore, it can be easily found that the hardness of textured surface is higher than smooth surface after laser treatment, which indicates that the laser treatment is able to improve the hardness of surface. Due to the quench hardening to the surface material induced by laser marking, precipitated phases are formed on the surface and the hardness of the surface is

enhanced directly. The variation of hardness of textured surface with different laser process parameters also shows the effect of microstructure on the surface to the hardness.

As shown in **Figure 6a**, it is apparent that the hardness of grating grooves surface with low texture spacing (≤ 50 μm) is higher than that of lined grooves surface. However, the hardness of lined grooves surface and grating grooves surface both decrease with the increasing of texture spacing. This is because the number of microstructures on unit area of the surface decreases with the increase of texture spacing, which will decrease the load carrying capacity of textured surface per unit area and decrease the hardness of the surface directly. With the texture spacing of surface increase from 75 μm to 100 μm, due to the decrease of the number of microstructures on unit area of the surface further reduces, the load carrying capacity of textured surface per unit area decreases. Therefore, the hardness of textured surface (grating grooves surface and lined grooves surface) is a little lower than that of smooth surface. The variation of hardness of textured surface indicates that the microstructure on the surface has a great effect to the hardness of the fabricated surface. Moreover, it is proved that the load carrying capacity of the grating grooves surface with low textures spacing (< 50 μm) is better than the lined grooves surface. With the increase of textures spacing, the number of microstructures on unit area of the grating grooves surface become smaller than that of lined grooves surface. Thus, the grating grooves surface shows lower hardness than lined grooves surface.

From the SEM image presented in the inset of **Figure 6b**, obviously the laser stay time on the surface and laser displacement gradually decrease as the laser frequency increase to 5000 Hz, leading to the decrease of melted degree of material. The irregular milky protrusion microfeatures are produced on the surface. Whereas at higher laser frequency, the melted degree of material is so low that melted material is unable to flock together. The low melted degree of

material also lead to the difficulty of individually constructing microstructure of melted material. Therefore, micro-pores pattern is produced on the surface by laser impacting force. Moreover, due to the extremely low melted degree of material, the integrity of textured surface is bad. Due to the modification of surface topography, the hardness of the surface decreases gradually with increasing laser frequency. **Figure 6c** shows the variations of hardness of grating grooves surface with laser scanning speed. With the increase of scanning speed (≥ 100 mm/s), the distance between two laser beams gradually increases, which leads to the increase of the distance between each melted spot. It is hard for the melted material around each melted spot to flock together. Thus, irregular milky protrusion microstructure is formed on the surface. Due to the change of the microfeatures of textured surface, the hardness of grating grooves surface has a decrease with the increasing of scanning speed from 50 to 100 mm/s and reached a minimum of 178 HV at the scanning speed of 100 mm/s. As the scanning speed continuously increases, the milky protrusion microstructure is more uniform and the number of microstructures on unit area of the surface increases, which could increase the load carrying capacity of textured surface per unit area. Therefore, the hardness of textured surface increases rapidly with increasing scanning speed. As shown in **Figure 6d**, the laser scanning times cannot change the degree of quench hardening induced by laser marking but the microstructure on the surface. Furthermore the microstructure of the surfaces treated by different laser scanning times is similar. Thus, the hardness of the textured surface has not a relatively great fluctuation with the increase of laser scanning times.

Due to the increase of the laser scanning times, the microstructure on the surface becomes bigger and more regular than before (**Figure 3c**), which increase the load carrying capacity of microstructure and the number of microstructures on unit area of the surface. Thus, the hardness of the surface increases. As continuously increase the scanning times to 4 (**Figure 3d**), the

microstructure turns to be more regular, while the diameter deceases. Although the number of microstructures on unit area of the surface has a slight increase, the load carrying capacity of microstructure decreases, leading to the hardness decrease of the surface.

The hardness test not only proves that the hardness of the surface can be improved after laser marking treatment, but also indicates that the microstructure on the surface has a great effect to the hardness of the surface. The shape of microstructure and the number of microstructures on unit area of the surface are crucial factors. The shape of microstructure with high load carrying capacity and great number of microstructures per unit area on the treated surface would lead to the higher hardness of the surface than others. On the contrary, the hardness of the textured surface would be low and even lower than that of untreated surface. Thus, accurately modulating the roughness structures on the surface is important and essential in the practical applications. When the number of microstructures on unit area of the surface is same, it is considered that the load carrying capacity of grating grooves structure is better than that of lined grooves structure and milky protrusion structure. Through laser marking treatment fabricating proper roughness structure on the surface of Al alloy, the hardness of Al alloy is able to be further enhanced. The hardness of textured surface treated under different processing parameters is in the range of 170-260 HV. Thus, compared with the smooth surface (185 HV), the maximum increase of hardness of these textured surfaces treated by this method reaches to 40 %.

**Figure 7a** and **b** show the curves of the dynamic friction coefficients of lined grooves and grating grooves surfaces with texture spacing against steel ball friction pair at a constant sliding speed of 16 mm/s and load of 1.65 N at room temperature. Clearly, the friction coefficient of the smooth surface sharply increases to about 0.55. Then it has fluctuations. While the textured surfaces (both lined grooves and grating grooves surfaces) show low and stable friction

coefficients at the beginning. The reason is that the microstructure on the surface can increase the load carrying capacity of the surface and reduce the friction force between the surface and steel ball. Therefore, the friction coefficient of surface can be reduced by constructing roughness structure on the surface. However, as shown in Figure 7a and b, the friction coefficient of texture surfaces increases after some sliding time. It is considered that the roughness structure of the textured surface is gradually worn during sliding friction and finally could not effectively decrease the friction between two surfaces. The sliding time before the friction coefficient increased sharply is seen as the wear life. Thus, it is easily seen that the wear life of textured surface treated under different processing parameters are different. The wear life of textured surface will affect the friction resistance of the surface. As shown in **Figure 7a**, it can be easily found that the wear life of the lined grooves surface with texture spacing of 100 μm is the highest of all, and the lined grooves surface with texture spacing of 50 and 150 μm has the same wear life. The wear life of lined grooves surface with texture spacing of 75 μm is the lowest. Compared with lined grooves surface, the grating grooves surfaces have higher wear life (**Figure 7b**), indicating that the friction resistance of grating grooves surface is better than that of lined grooves surface. The wear life of the surface decreases with the increasing of texture spacing, showing more regular variation of wear life of the grating grooves surface than that of lined grooves surface. Furthermore, the stable friction coefficient of the surface increases with the increment of texture spacing. It is considered that the microstructure on the surface has not been worn out after test.

When the grating grooves surface treated at the laser frequency of 5000 Hz, the irregular milky protrusion microfeatures are produced on the surface. The wear life of the surface dramatically decreases (**Figure 7c**), which means that it is easy for the milky protrusion to be worn out and

the wear resistance of the surface is poor. However, the wear life of the surface increases at higher laser frequency. That is because, compared with convex structure, it is difficult for concave structure on Al alloy surface to be destroyed. Though the wear life of the surface is the highest of all, the integrity of the surface is very bad and uncontrolled. In other words, it is hard for facile operation in the large scale and engineering applications. As shown in **Figure 7d**, the wear life of grating surface decreases with the increasing of laser scanning speed. The variation of the wear life of the grating grooves surface with laser frequency and scanning speed also indicates that the wear life of milky protrusion structure is lower than that of grating grooves structure. Furthermore, with the increasing of scanning time to 2, the roughness structure of the grating grooves surface is more easily worn out. As the scanning times increases to 4, the wear life of the textured surface increases (**Figure 7e**). Therefore, the regular microstructure on the surface would have long wear life.

The friction test shows that the friction coefficient of surface can be remarkably reduced by constructing roughness structure on the surface. Compared with smooth surface (0.562), the decrease of friction coefficient of textured surface can reach to 80%. Thus, it is an efficient method to reduce the friction coefficient and improve the friction resistance of surface. However, to the textured surface, the wear life of microstructure on the surface is much more important than friction coefficient and should be paid attention. Different microstructure on the textured surface has different wear life, which will affect the friction resistance of Al alloy. Compared with lined grooves structure and milky protrusion structure, the grating grooves structure on the Al alloy surface has a longer wear life, which indicates that the friction resistance of grating grooves surfaces of Al alloy is better than others. Moreover, due to the regular variation of wear

life of the grating grooves surface with textures spacing, it is easy for grating grooves surface to be applied in engineering.

**Figure 8** shows the variations of wear volume of the textured surface treated by different processing parameters. It can be easily found that the wear volume of textured surfaces is lower than that of smooth surface. It indicates that the friction resistance of textured surface can be enhanced by laser marking treatment. As shown in **Figure 8a**, the variations of wear volume of the lined grooves surface decreases with the increase of the texture spacing from 25 to 50 μm. Then it drops very slowly with increasing texture spacing. Clearly the wear volume of surface is not only affected by the hardness of the surface, but also influenced by the wear life of microstructure on the surface. On the contrary, the variations of wear volume of grating grooves surface increases with increasing texture spacing. With the increase of the laser frequency, the wear volume of grating grooves surface decreases (**Figure 8b**). From the variation of wear volume shown in **Figure 8c**, it can be observed that the wear volume of textured surface has an increase with the increase of the laser scanning speed from 50 to 100 mm/s and falls dramatically with the increasing of the laser scanning speed from 100 to 200 mm/s. The variations of wear volume of the textured surface with scanning times are shown in **Figure 8d**. It can be easily found that the wear volume decreases with the increase of the scanning times.

The wear volume of textured surfaces after friction experiment indicates that the friction resistance of the textured surface treated by this method is much better than that of smooth surface. The wear volume of smooth surface is 0.57 mg, but the minimum of the wear volume of the fabricated surface is 0.14 mg. In other words, the wear volume of fabricated surface could be one fifth lower than that of smooth surface. Moreover, the variation of wear volume of textured surface treated by different processing parameters proves that the hardness of the surface and the

wear life of microstructure on the textured surface have a combined effect on the friction resistance of the textured surface. The textured surface with high hardness and long wear life microstructure would have excellent friction resistance. Therefore, the friction resistance of the textured surface can be further improved by constructing proper roughness structure on the surface. Compared with other textured surfaces, the friction resistance of grating grooves surface with low textures spacing is much better. And the grating grooves surface of Al alloy will have an extensive application in engineering.

In the following, the antifriction mechanism of the textured surface is further investigated. SEM images of the worn surfaces of the smooth surface and textured surfaces are shown in **Figure 9**. As shown in **Figure 9a and b**, it can be easily observed that the microstructure on the lined grooves surface is worn out after friction test, showing short wear life of microstructure. The smooth surface seems as smooth as the textured surface after the friction test. But actually, the smoothness of smooth surface and lined grooves surface are different after the test. From the high-magnification SEM image shown in **Figure 9d and e**, it is obvious that the smooth surface is very uneven and many scratches appear on the surface. On the contrary, the lined grooves surface is comparatively smooth after the test. The phenomenon shows that the wear debris of the textured surface treated by laser marking can behave as spacers and form a lubrication film to reduce friction between steel ball and the surface. The wear debris of smooth surface will increase the friction between two surfaces. Therefore, it is proved that the friction resistance of Al alloy can be enhanced though laser marking constructing microstructure on the surface. As shown in **Figure 9c and f**, obviously, the microstructure on the grating grooves surface is still remained after the test, which is in good agreement with the curves of the dynamic friction coefficients of the surface and also proved that grating grooves structure has longer wear life

than others. Thus, it is considered that the textured surface of Al alloy with grating grooves structure has an excellent friction resistance.

## CONCLUSIONS

Lined and grating grooves texture were produced on AA7075 Al alloy surface by a simple, convenient, low cost and able to process large area method. The effect of processing parameters on microstructure, corrosion resistance to seawater, hardness and friction resistance of textured surface has been studied. Through adjusting the processing parameters (laser frequency, laser scanning speed, laser scanning times, texture spacing), roughness structures on the surface can be accurately modulated. Compared with untreated Al alloy, the corrosion resistance to seawater of textured surface treated by this method could be significantly enhanced. Moreover, it is proved that the hardness of the surface can be improved after the treatment. More importantly, tribological measurements illustrated that the friction resistance of the surface can be enhanced by this method and showing that the microstructure on the surface will affect the friction resistance of the textured surface. Therefore, through this convenient method constructing proper microstructure (the textured surface with grating grooves structure and low textures spacing) on the surface, the corrosion resistance to seawater, hardness and friction resistance of Al alloy could be dramatically improved simultaneously, which would extend the applications of Al alloy in engineering field.



## ACKNOWLEDGMENTS

This work was supported by the National Key Scientific Program-Nanoscience and Nanotechnology (2011CB933700), and National Natural Science Foundation of China

(21073197). X.J.H. acknowledges the CAS Institute of Physical Science, University of Science and Technology of China (2012FXCX008), for financial support.

**Figure Captions:**

**Figure 1**. (a) Schematic process of the fabrication of roughness structure on Al alloy surface by laser marking machine; (b) schematic process of the formation of roughness structure.

**Figure 2**. (a) The treated Al plate; (b) SEM image of untreated Al alloy surface morphology; (c) SEM image of lined grooves surface morphology (textures spacing of 50 μm, frequency of 2500 Hz, scanning speed of 50 mm/s); (d) SEM image of grating grooves surface morphology (textures spacing of 50 μm frequency of 2500 Hz, scanning speed of 50 mm/s).

**Figure 3**. Low-magnification SEM image of grating grooves surface (textures spacing of 50 μm) morphology treated by different laser processing parameters: (a) laser frequency of 5000 Hz, scanning speed of 50 mm/s, scanning times of 1; (b) frequency of 2500 Hz, scanning speed of 150 mm/s, scanning times of 1; (c) frequency of 2500 Hz, scanning speed of 50 mm/s, scanning times of 2; (d) frequency of 2500 Hz, scanning speed of 50 mm/s, scanning times of 4.

**Figure 4**. XPS spectra of untreated and textured surfaces (grating grooves surface, textures spacing of 50 μm, frequency of 2500 Hz, scanning speed of 50 mm/s, scanning times of 1, 2 and 4 respectively) of (a) survey; (b)Mg 2p; (c)Al 2p; (d)Si 2p; (e)Zn 2p3; (f)Cu 2p.

**Figure 5**. (a) Smooth surface corresponding to the sample; (b) textured surface corresponding to the sample; (c) Smooth surface corresponding to the sample soaked in seawater after 20 days; (d) textured surface corresponding to the sample soaked in seawater after 20 days; (e) SEM image of smooth surface; (g) SEM image of textured surface.

**Figure 6**. Hardness distributions of sample surface treated by different laser processing parameters: (a) lined grooves surface and grating grooves surface, frequency of 2500 Hz, scanning speed of 50 mm/s, scanning times of 1; (b) grating grooves surface, textures spacing of 50 μm, scanning speed of 50 mm/s, scanning times of 1; (c) grating grooves surface, textures spacing of 50 μm, frequency of 2500 Hz, scanning times of 1; (d) grating grooves surface, textures spacing of 50 μm, frequency of 2500 Hz, scanning speed of 50 mm/s, scanning times of 1, 2, 4. Scale bar: 50 μm

**Figure 7**. Dynamic friction coefficient of sample surface treated by different laser processing parameters (load of 165 N, sliding speed of 16 mm/s): (a) lined grooves surface, frequency of 2500 Hz, scanning speed of 50 mm/s, scanning times of 1(A: untreated; texture spacing of B: 25 μm; C:50 μm; D: 75 μm; E: 100 μm; F: 150 μm); (b) grating grooves surface, frequency of 2500 Hz, scanning speed of 50 mm/s, scanning times of 1(A: untreated; texture spacing of B: 25 μm; C:50 μm; D: 75 μm; E: 100 μm; F: 150 μm); (c) grating grooves surface, textures spacing of 50 μm, scanning speed of 50 mm/s, scanning times of 1; (d) grating grooves surface, textures spacing of 50 μm, frequency of 2500 Hz, scanning times of 1; (e) grating grooves surface, textures spacing of 50 μm, frequency of 2500 Hz, scanning speed of 50 mm/s.

**Figure 8**. Wearing volume of sample surface treated by different laser processing parameters(load of 165N,sliding speed of 16 mm/s,): (a) lined grooves surface and grating grooves surface, frequency of 2500 Hz, scanning speed of 50 mm/s, scanning times of 1; (b) grating grooves surface, textures spacing of 50 μm, scanning speed of 50 mm/s, scanning times

of 1; (c) grating grooves surface, textures spacing of 50 μm, frequency of 2500 Hz, scanning times of 1; (d) grating grooves surface, textures spacing of 50 μm, frequency of 2500 Hz, scanning speed of 50 mm/s, scanning times: 1, 2, 4.

**Figure 9**. SEM images of the middle of the worn surfaces under dry sliding for Al alloy: (a and d) untreated surface; (b and e) lined grooves surface; (c and f) grating grooves surface.

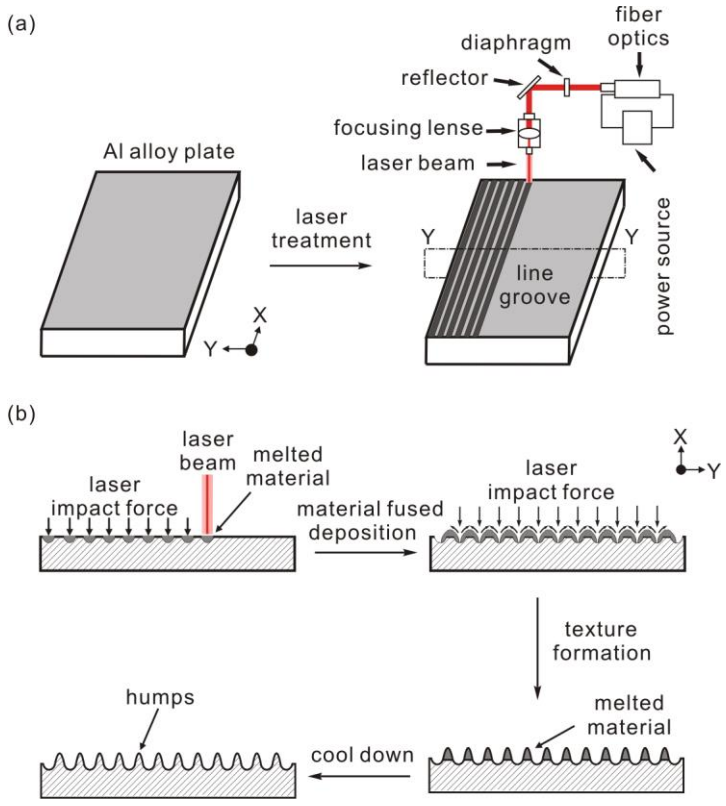


**Figure 1**. (a) Schematic process of the fabrication of roughness structure on Al alloy surface by laser marking machine; (b) schematic process of the formation of roughness structure.

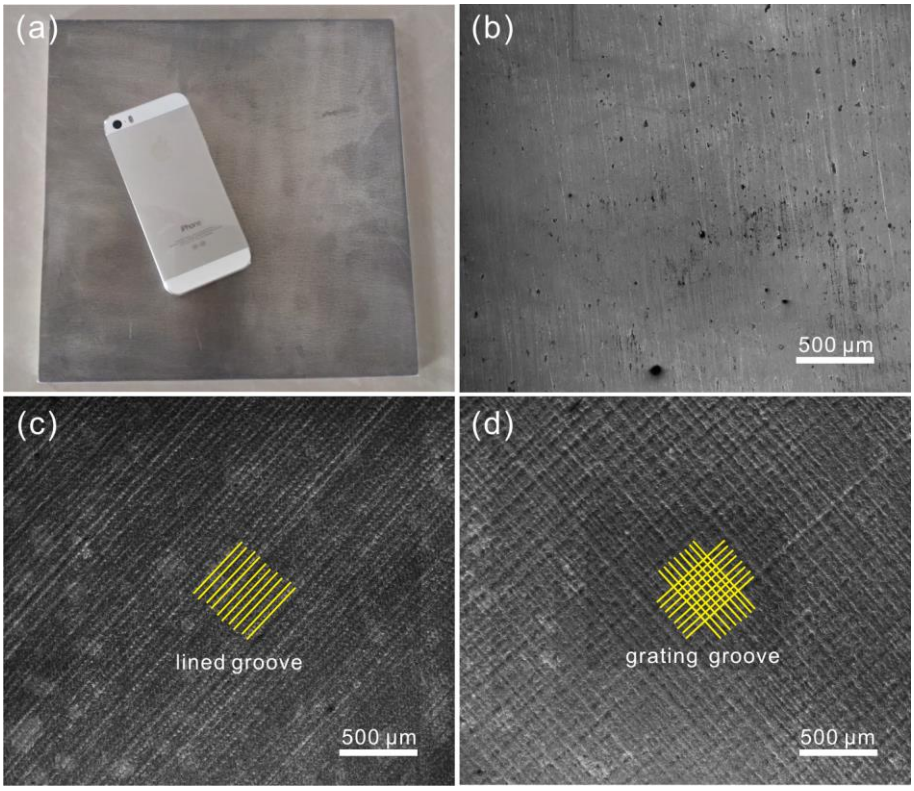


**Figure 2**. (a) The treated Al alloy plate; (b) SEM image of untreated Al alloy surface morphology; (c) SEM image of lined grooves surface morphology (textures spacing of 50 μm, frequency of 2500 Hz, scanning speed of 50 mm/s); (d) SEM image of grating grooves surface morphology (textures spacing of 50 μm frequency of 2500 Hz, scanning speed of 50 mm/s).

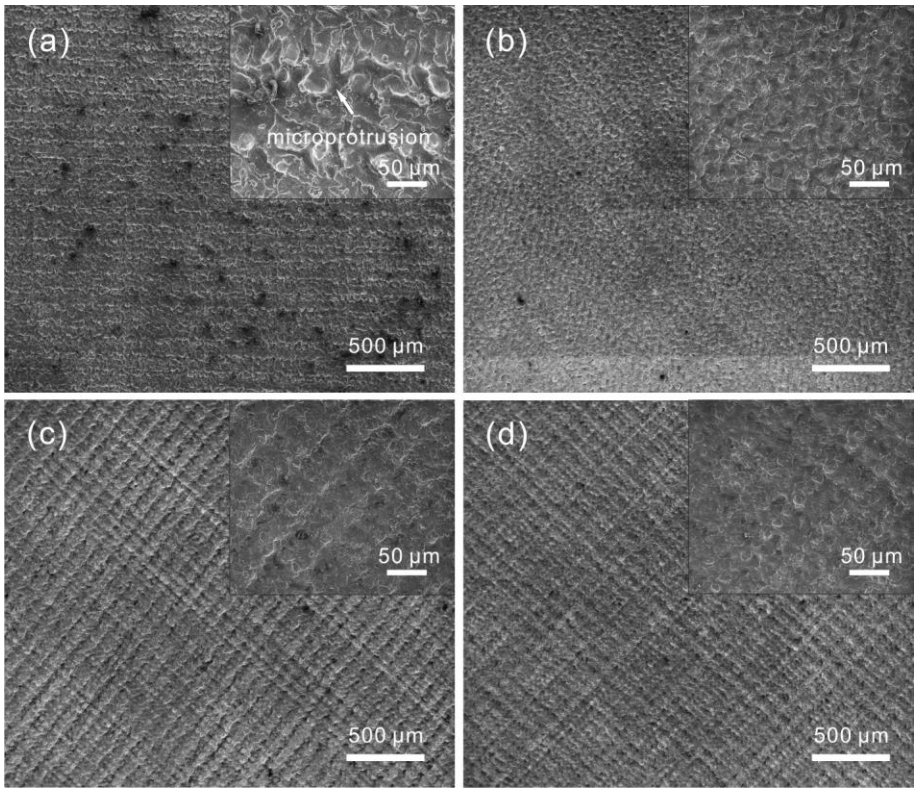


**Figure 3**. Low-magnification SEM image of grating grooves surface (textures spacing of 50 μm) morphology treated by different laser processing parameters: (a) laser frequency of 5000 Hz, scanning speed of 50 mm/s, scanning times of 1; (b) frequency of 2500 Hz, scanning speed of 150 mm/s, scanning times of 1; (c) frequency of 2500 Hz, scanning speed of 50 mm/s, scanning times of 2; (d) frequency of 2500 Hz, scanning speed of 50 mm/s, scanning times of 4.

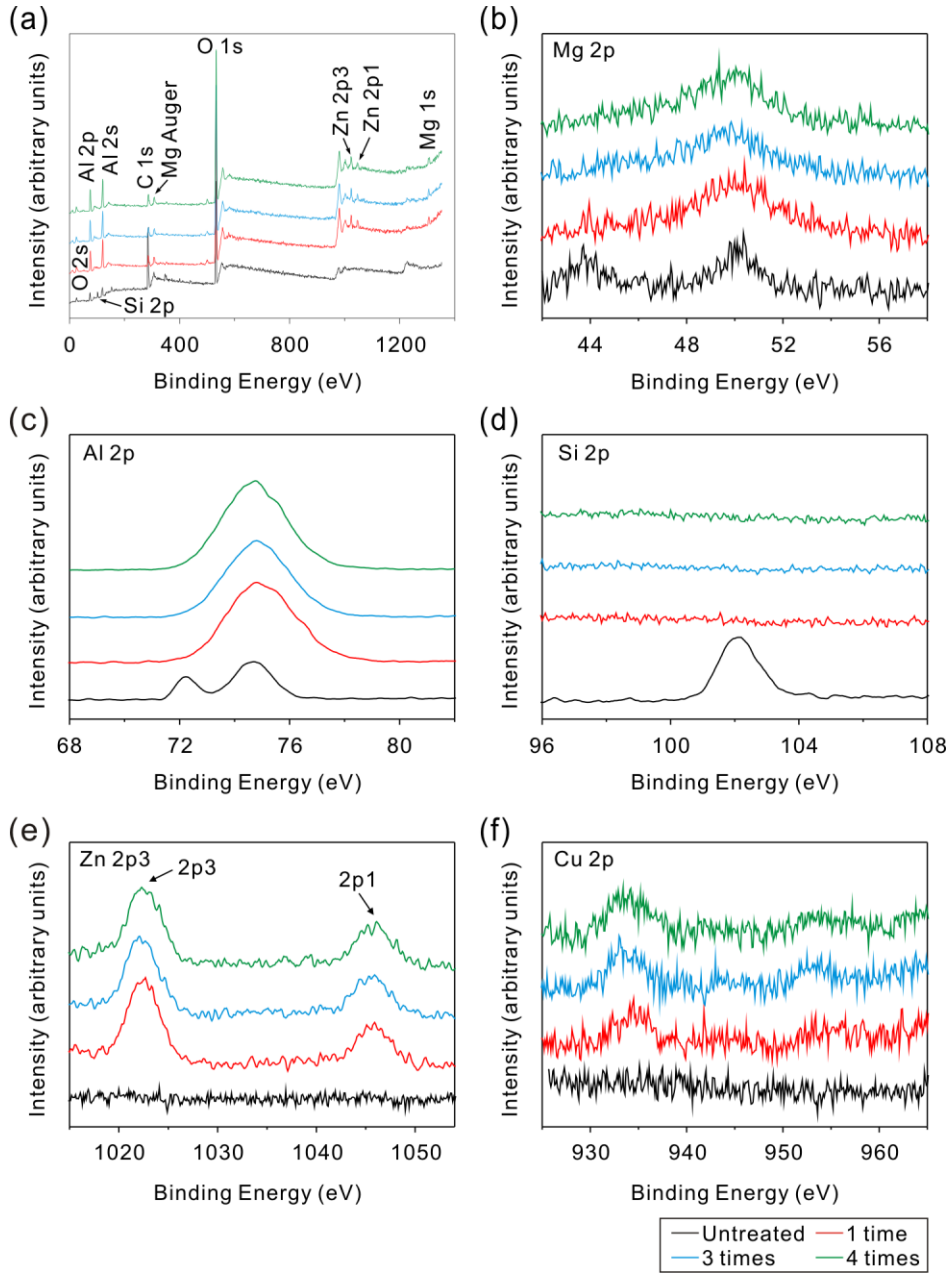


**Figure 4**. XPS spectra of untreated and textured surfaces (grating grooves surface, textures spacing of 50 μm, frequency of 2500 Hz, scanning speed of 50 mm/s, scanning times of 1, 2 and 4 respectively) of (a) survey; (b)Mg 2p; (c)Al 2p; (d)Si 2p; (e)Zn 2p3; (f)Cu 2p.

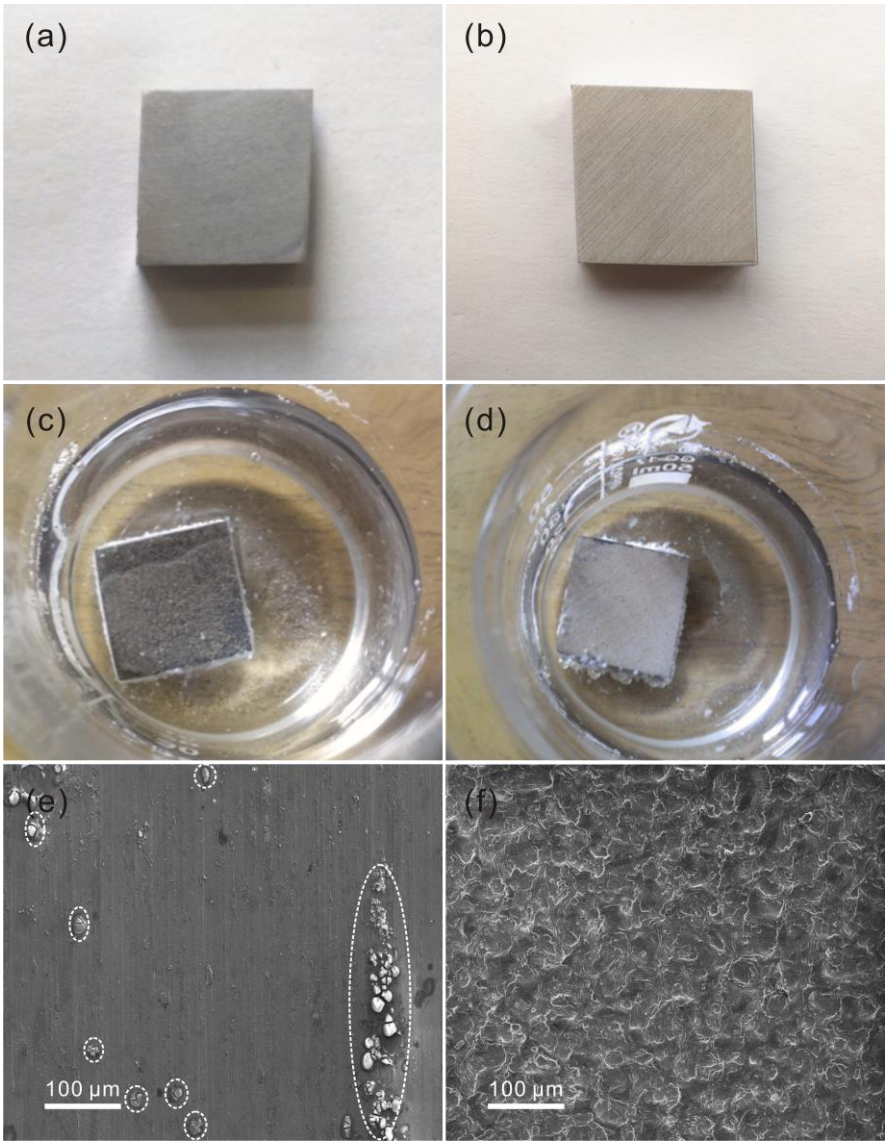


**Figure 5**. (a) Smooth surface corresponding to the sample; (b) textured surface corresponding to the sample; (c) Smooth surface corresponding to the sample soaked in seawater after 20 days; (d) textured surface corresponding to the sample soaked in seawater after 20 days; (e) SEM image of smooth surface; (g) SEM image of textured surface.

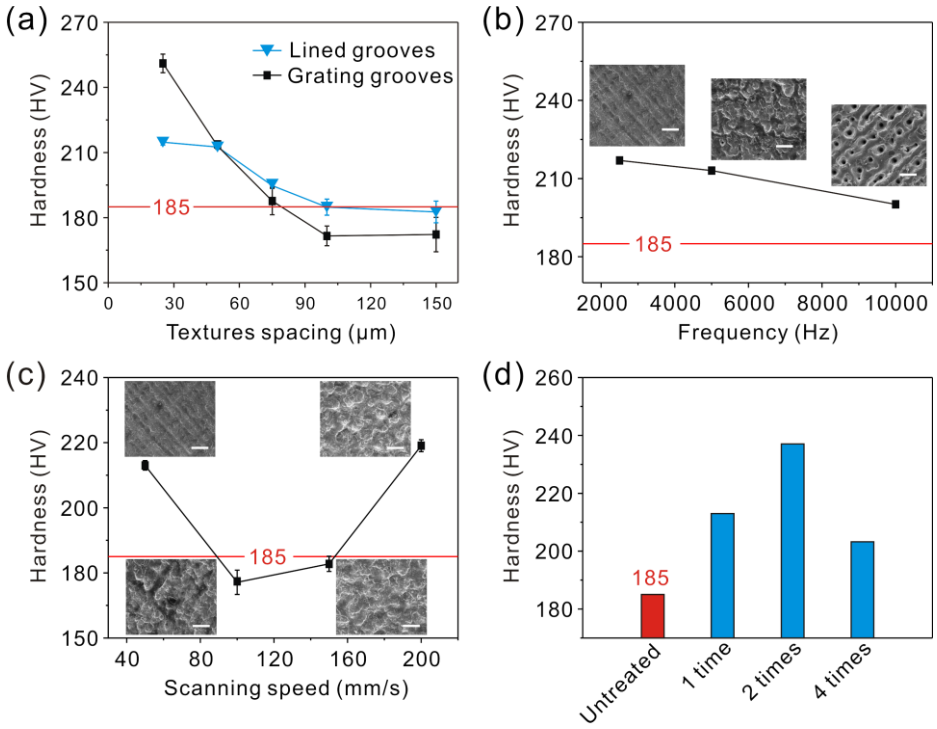


**Figure 6**. Hardness distributions of sample surface treated by different laser processing parameters: (a) lined grooves surface and grating grooves surface, frequency of 2500 Hz, scanning speed of 50 mm/s, scanning times of 1; (b) grating grooves surface, textures spacing of 50 μm, scanning speed of 50 mm/s, scanning times of 1; (c) grating grooves surface, textures spacing of 50 μm, frequency of 2500 Hz, scanning times of 1; (d) grating grooves surface, textures spacing of 50 μm, frequency of 2500 Hz, scanning speed of 50 mm/s, scanning times of 1, 2, 4. Scale bar: 50 μm.

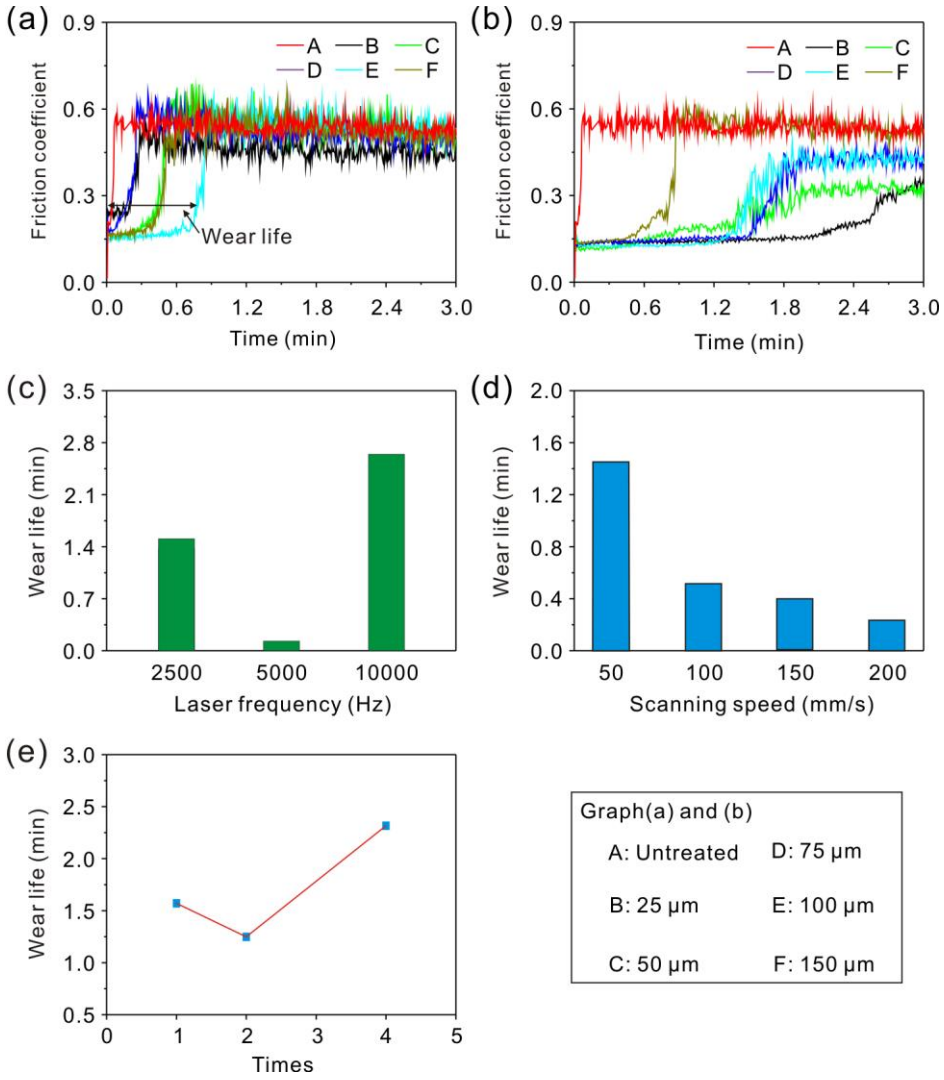


**Figure 7.** Dynamic friction coefficient of sample surface treated by different laser processing parameters (load of 165 N, sliding speed of 16 mm/s): (a) lined grooves surface, frequency of 2500 Hz, scanning speed of 50 mm/s, scanning times of 1(A: untreated; texture spacing of B: 25 μm; C:50 μm; D: 75 μm; E: 100 μm; F: 150 μm); (b) grating grooves surface, frequency of 2500 Hz, scanning speed of 50 mm/s, scanning times of 1(A: untreated; texture spacing of B: 25 μm; C:50 μm; D: 75 μm; E: 100 μm; F: 150 μm); (c) grating grooves surface, textures spacing of 50 μm, scanning speed of 50 mm/s, scanning times of 1; (d) grating grooves surface, textures spacing of 50 μm, frequency of 2500 Hz, scanning times of 1; (e) grating grooves surface, textures spacing of 50 μm, frequency of 2500 Hz, scanning speed of 50 mm/s.

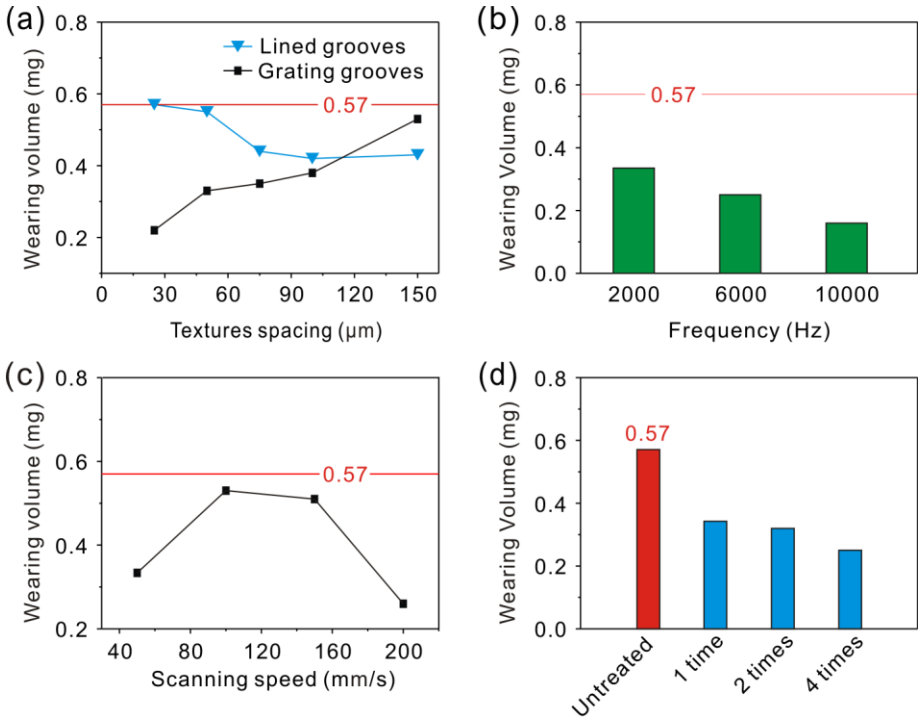


**Figure 8**. Wearing volume of sample surface treated by different laser processing parameters(load of 165N,sliding speed of 16 mm/s,): (a) lined grooves surface and grating grooves surface, frequency of 2500 Hz, scanning speed of 50 mm/s, scanning times of 1; (b) grating grooves surface, textures spacing of 50 μm, scanning speed of 50 mm/s, scanning times of 1; (c) grating grooves surface, textures spacing of 50 μm, frequency of 2500 Hz, scanning times of 1; (d) grating grooves surface, textures spacing of 50 μm, frequency of 2500 Hz, scanning speed of 50 mm/s, scanning times: 1, 2, 4.

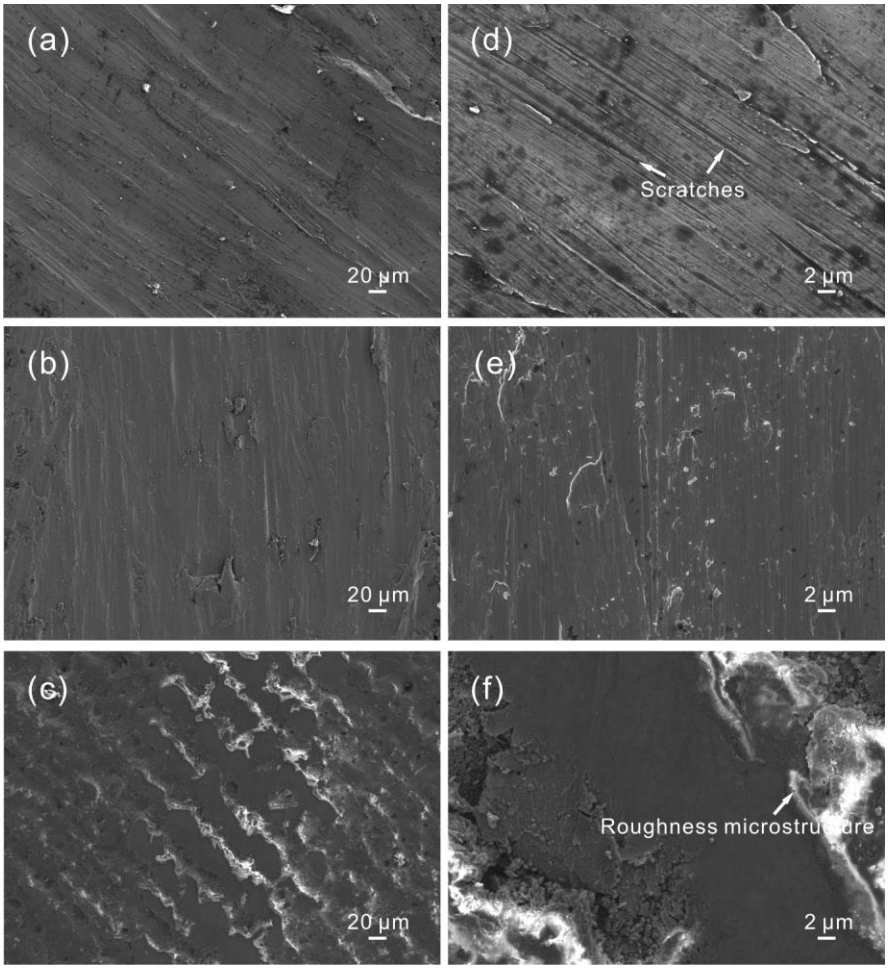


**Figure 9**. SEM images of the middle of the worn surfaces under dry sliding for Al alloy: (a and d) untreated surface; (b and e) lined grooves surface; (c and f) grating grooves surface.

**Table 1**. Surface element contents calculated from XPS survey spectra.

| | C (At. %) | O (At. %) | Al (At. %) | Mg (At. %) | Si (At. %) | Zn (At. %) | Cu (At. %) |
|---|---|---|---|---|---|---|---|
| Untreated | 59.24 | 29.64 | 7.56 | 0.89 | 2.67 | None | None |
| Scanning 1 times | 11.60 | 64.34 | 20.16 | 2.30 | None | 1.28 | 0.32 |
| Scanning 2 times | 11.30 | 64.97 | 20.39 | 1.55 | None | 1.42 | 0.36 |
| Scanning 4 times | 12.17 | 63.34 | 21.16 | 1.65 | None | 1.28 | 0.40 |

## REFERENCES


1. J. R. Davis, *Asm International*, 1999, 1-43.
2. A. Laurino, E. Andrieu, J. P. Harouard, G. Odemer, J. C. Salabura and C. Blanc, *Materials & Design*, 2014, **53**, 236-249.
3. A. Astarita, C. Bitondo, A. Squillace, E. Armentani and F. Bellucci, *Surface And Interface Analysis*, 2013, **45**, 1610-1618.
4. T. Knych, M. Piwowarska-Uliasz and P. Uliasz, *Archives of Metallurgy and Materials*, 2014, **59**, 339-343.
5. W. S. Miller, L. Zhuang, J. Bottema, A. Wittebrood, P. De Smet, A. Haszler and A. Vieregge, *Materials Science and Engineering a-Structural Materials Properties Microstructure and Processing*, 2000, **280**, 37-49.
6. J. Xiao and S. Chaudhuri, *Electrochimica Acta*, 2011, **56**, 5630-5641.
7. H. B. I. John, *Arabian Journal For Science And Engineering*, 2014, **39**, 1409-1415.
8. Y. S. Zou, K. Zhou, Y. F. Wu, H. Yang, K. Cang and G. H. Song, *Vacuum*, 2012, **86**, 1141-1146.
9. B. A. Shaw, G. D. Davis, T. L. Fritz, B. J. Rees and W. C. Moshier, *Journal Of The Electrochemical Society*, 1991, **138**, 3288-3295.
10. N. Dimitrov, J. A. Mann and K. Sieradzki, *Journal Of The Electrochemical Society*, 1999, **146**, 98-102.
11. R. G. Buchheit, R. P. Grant, P. F. Hlava, B. McKenzie and G. L. Zender, *Journal Of The Electrochemical Society*, 1997, **144**, 2621-2628.
12. P. Schmutz and G. S. Frankel, *Journal Of The Electrochemical Society*, 1998, **145**, 2295-2306.
13. W. C. Moshier, G. D. Davis, J. S. Ahearn and H. F. Hough, *Journal Of The Electrochemical Society*, 1986, **133**, 1063-1064.
14. M. Metikos-Hukovic, R. Babic and Z. Grubac, *Journal Of The Electrochemical Society*, 2009, **156**, C435-C440.
15. J. P. Pathak and S. Mohan, *Bulletin Of Materials Science*, 2003, **26**, 315-320.
16. P. Liu, E. Domingue, D. C. Ayers and J. Song, *ACS applied materials & interfaces*, 2014, **6**, 7141-7152.
17. Q. X. Zhang, Y. X. Chen, Z. Guo, H. L. Liu, D. P. Wang and X. J. Huang, *ACS applied materials & interfaces*, 2013, **5**, 10633-10642.
18. H. Bostanci, V. Singh, J. P. Kizito, D. P. Rini, S. Seal and L. C. Chow, *ACS applied materials & interfaces*, 2013, **5**, 9572-9578.
19. N. Ghosh, A. V. Singh and A. A. Vaidya, *ACS applied materials & interfaces*, 2013, **5**, 8869-8874.
20. M. Ksiazek, A. Tchorz and L. Boron, *Journal Of Materials Engineering And Performance*, 2014, **23**, 1635-1640.
21. T. J. Kang, J.-G. Kim, H.-Y. Lee, J.-S. Lee, J.-H. Lee, J.-H. Hahn and Y. H. Kim, *International Journal of Precision Engineering and Manufacturing*, 2014, **15**, 889-894.
22. L. Li and G. M. Swain, *ACS applied materials & interfaces*, 2013, **5**, 7923-7930.
23. E. Husain, T. N. Narayanan, J. J. Taha-Tijerina, S. Vinod, R. Vajtai and P. M. Ajayan, *ACS applied materials & interfaces*, 2013, 130507093329006.
24. J. Mukherjee, S. Chakraborty, S. Chakravarty, A. Ranjan and P. K. Das, *Ceramics International*, 2014, **40**, 6639-6645.

25. C. Guo, R. Yao, H. Kong, J. Chen and J. Zhou, *Surface and Coatings Technology*, 2014, **246**, 40-45.
26. E. V. Skorb, D. Fix, D. V. Andreeva, H. Möhwald and D. G. Shchukin, *Advanced Functional Materials*, 2009, **19**, 2373-2379.
27. S. M. Lari Baghal, M. Heydarzadeh Sohi and A. Amadeh, *Surface and Coatings Technology*, 2012, **206**, 4032-4039.
28. J. Qu, H. Xu, Z. Feng, D. A. Frederick, L. An and H. Heinrich, *Wear*, 2011, **271**, 1940-1945.
29. Z. C. Guo, R. M. Wang and Y. F. Wang, *Transactions of the IMF*, 2008, **86**, 55-61.
30. S. Kalainathan, S. Sathyajith and S. Swaroop, *Optics And Lasers In Engineering*, 2012, **50**, 1740-1745.
31. E. E. Ghadim, N. Rashidi, S. Kimiagar, O. Akhavan, F. Manouchehri and E. Ghaderi, *Applied Surface Science*, 2014, **301**, 183-188.
32. B. S. Yilbas, *Surface and Coatings Technology*, 2013, **236**, 315-319.
33. K. Miyake, M. Nakano, A. Korenaga, H. Mano and Y. Ando, *Journal of Physics D: Applied Physics*, 2010, **43**, 465302.
34. E. Brinksmeier, O. Riemer and S. Twardy, *International Journal of Machine Tools and Manufacture*, 2010, **50**, 425-430.
35. E. Uhlmann, T. B. Klein, L. Hochschild and C. Bäcker, *Procedia Engineering*, 2011, **19**, 363-370.
36. K. Steinhoff, W. Rasp and O. Pawelski, *Journal Of Materials Processing Technology*, 1996, **60**, 355-361.
37. P. Traverso, A. M. Beccaria and G. Poggi, *British Corrosion Journal*, 1995, **30**, 227-231.
38. H. Ezuber, A. El-Houd and F. El-Shawesh, *Materials & Design*, 2008, **29**, 801-805.

## Graphical Abstract

Through a simple, convenient, efficient, and low cost laser marking approach, microstructures (lined and grating grooves textures) on the large scale engineering material surface, i.e., AA7075 Al alloy, have been successfully fabricated. Compared with untreated Al alloy, the corrosion resistance to seawater, hardness and wear resistance of the textured surface treated by this method could be simultaneously improved, which presented a great perspective concerning to the engineering field.